RSC Advances

ROYAL SOCIETY OF CHEMISTRY

www.rsc.org/advances

Graphical Abstract

Nanomolar Zinc detection and subsequent pyrophosphate sensing in physiological medium using a benzothiazole modified conjugated ligand and their application in paper strip and live cell imaging is demonstrated.

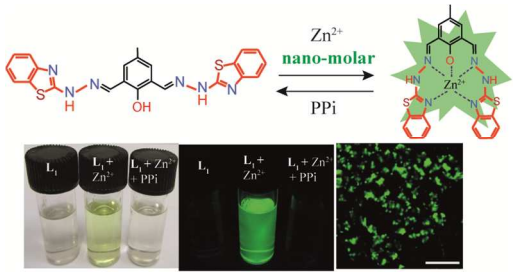

Journal Name

RSCPublishing

ARTICLE

Nanomolar Zn(II) Sensing and Subsequent PPi Detection in Physiological Medium and Live Cells with A Benzothiazole Functionalized Chemosensor

Abhijit Gogoi,[a] Sandipan Mukherjee,[b] Aiyagari Ramesh,*[b] and Gopal Das*[a]

Cite this: DOI: 10.1039/xoxxoooooox

Received ooth January 2012,
Accepted ooth January 2012

DOI: 10.1039/xoxxoooooox

www.rsc.org/

New fluorescent chemosensor ($\mathbf{L_1}$) exhibit relay recognition of Zn^{2+} and pyrophosphate anion in mixed buffer solution at physiological pH. The probe exhibit excellent Zn^{2+} induced turn-on fluorescence, even as low as 1 nM (LOD = 71 ppb). Further, addition of pyrophosphate ion led to quenching of fluorescence signal of $\mathbf{L_1}$-Zn^{2+} ensemble. The sensitive fluorescence behavior of the $\mathbf{L_1}$ rendered a useful probe for in vitro assays of the intracellular Zn^{2+} and PPi ion in model human cell line.

Introduction

Development of molecular fluorescence-based chemosensors for metal ions has emerged as an important field of research owing to the central role of metal in biology, environment and chemical process.[1] Fluorescent chemosensors are widely preferred over other optical sensors based on their high sensitivity, ease of handling, robustness and the possibility of real-time monitoring with fast response time.[2-3] Amongst the metal ions, zinc ion sensing in aqueous environment is assuming considerable importance due to the fundamental role of the metal in a plethora of biological processes, such as gene transcription, regulation of metalloenzymes, neural signal transmission and apoptosis.[4-9] Zinc is acknowledged as the second most abundant metal ion in human body after iron and is commonly associated with proteins where it bears structural and catalytic implications.[10] Besides the fixed form of cellular zinc, pools of labile zinc is found in the pancreas,[11] central nervous system,[12] prostate,[13-14] intestine[15-16] and retina.[17] Deficiency of zinc ion has been implicated in grave ailments such as acrodermatitis enteropathica, impaired cognition, immune dysfunction and diarrhea, while an excess concentration has been known to cause superficial skin diseases, prostate cancer, diabetes and brain diseases.[18-19] The paucity of knowledge with regard to the physiological implications of cellular zinc homeostasis and the increasing need to unravel the role of Zn^{2+} in disease-related pathways has triggered the development of analytical tools for rapid and sensitive detection of the metal.[20-21] However, the inherent traits of zinc such as absence of any spectroscopic signature as well as neutral magnetism are considered as bottlenecks to apply common analytical techniques for detection. Furthermore, the toxic cadmium ion, which is analogous to zinc in electronic configuration mostly interferes in the detection of zinc ion. Given this predicament, selective, sensitive and rapid detection of zinc ions in complex milieu and in biological samples is in great demand.

In recent times, zinc chemosensing ensembles have emerged as secondary sensors towards various anions,[22-24] small molecule such as biothiols,[25] nitro aromatic compounds,[26-27] and amino acids.[28] Amongst the anion, sensing of biologically important pyrophosphate ($P_2O_7^{4-}$, PPi) is desirable as it plays a germane role in various biological process.[29-30] PPi is the product of ATP hydrolysis under cellular conditions and is a by-product of DNA replication and DNA sequencing.[31-32] Most importantly, the detection of PPi has also been considered to be important in cancer research.[33] Further, PPi detection has become an important issue for rheumatological disorder that originates due to the accumulation of crystals of calcium pyrophosphate dehydrates in the connective tissues.[34-37] The high solvation energy of PPi in water (ΔG^o = - 584 KJ mol^{-1})[38] and the presence of other competitive anions is a formidable challenge for detection of PPi in aqueous medium using receptors, which are based only on H-bonding interaction. Thus, certain transition metal chemosensor ensembles including Zn^{2+}, Cd^{2+} and Cu^{2+}, are being deployed to surmount this problem.[39-42] It is envisaged that such ensembles can provide the geometry and suitable orientation of the binding site for the anions, which have an inherent proclivity for binding the positive centred metal ions. Apart from this colorimetric/fluorimetric type sensors, bioluminescence[43] electrochemical[44] and ISFET[45] based sensors are also known in the literature.

Our research group has a longstanding interest in the design and development of chemosensors for the molecular recognition and sensing of various analytes.[46-49] Based on the aforementioned premise, herein we report the synthesis and photophysical properties of a benzothiazole based dipodal Schiff base chemosensor **L_1** (2,6-bis((E)-(2-(benzothiazol-2-yl)hydrazono)methyl)-4-methylphenol).

The benzothiazole unit acts as chelating ligand[46] and the dipodal Schiff base framework provide efficient binding for metal ion.[48, 50-53] The new chemosensor is highly selective towards Zn^{2+} ion with a detectable fluorescence response even with 1 nM Zn^{2+}. Furthermore, the chemosensor **L_1** rendered Zn^{2+} in the physiological milieu and the resultant **L_1**-Zn^{2+} ensemble responded specifically to pyrophosphate (PPi) anion through fluorescence quenching.

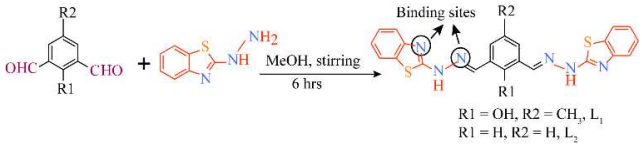

Scheme 1. Synthetic scheme of the receptors with the binding sites for guest metals.

Experimental Section

General Information and Materials

All the materials used for synthesis were procured from commercial suppliers. The absorption spectra were recorded on a Perkin-Elmer Lamda-750 UV-Vis spectrophotometer using 10 mm path length quartz cuvettes in the range 250-700 nm wavelength, while fluorescence measurements were conducted on a Horiba Fluoromax-4 spectrofluorometer using 10 mm path length quartz cuvettes with a slit width of 3 nm at 298 K. Mass spectra of **L_1** was obtained using Waters Q-ToF Premier mass spectrometer. NMR spectra were recorded on a Varian FT-400 MHz instrument as well as on a BRUKER-600 MHz and the chemical shifts were presented in parts per million (ppm) on the scale. The following abbreviations are used to describe spin multiplicities in ^{1}H NMR spectra: s = singlet; d = doublet; t = triplet; m = multiplet. IR spectra were recorded on a Perkin Elmer-Spectrum One FT-IR spectrometer with KBr disks in the range 4000-450 cm^{-1}.

Synthesis of L_1

Condensation of freshly prepared 2,6-Diformyl-4-methylphenol with 2-hydrazino benzothiazole for 4 hours yielded a yellowish precipitate, which was then filtered and washed with cold methanol to obtain pure **L_1** (Scheme 1). % Yield = 85. ^{1}H NMR of **L_1** (400 MHz, DMSO-d_6): 12.267 (bs, 1H), 8.484 (s, 2H), 7.727-7.753 (d, 2H), 7.561 (s, 2H), 7.354-7.229 (m, 4H), 7.128-7.091 (t, 2H), 2.319 (s, 3H). ^{13}C NMR (600 MHz): 166.58, 153.78, 133.41, 128.43, 126.28, 121.92, 121.66, 120.16, 20.12. ESI-MS (positive mode, m/z) Calculated [**L_1** + H^+] = 459.1062, found mass: 459.1042.

Similarly, condensation of 2,6-Diformyl-benzene with 2-hydrazino benzothiazole for 4 hours gives gave a yellowish type precipitate of **L_2**. % Yield = 80. ^{1}H NMR of **L_2** (400 MHz, DMSO-d_6): 12.353(bs, 1H), 8.181(s, 2H), 7.981(s, 1H), 7.801-7.603 (m, 4H), 7.528-7.454 (m, 3H), 7.310 (t, 2H), 7.125 (t, 2H). ^{13}C NMR: 167.180, 134.94, 129.12, 127.386, 126.059, 124.125, 121.765, 120.94. ESI-MS (positive mode, m/z) Calculated [**L_2** + H^+] = 429.1004, found mass: 429.0948.

UV−Vis and Fluorescence Spectral Studies

Stock solutions of various ions (1×10^{-3} M) were prepared in deionized water. Perchlorate or nitrate salts were used for metal ions while tetrabutyl/tetraethyl or sodium salts of the corresponding anions and nucleotides were used for the preparation of anion stock solutions. The stock solution of **L_1** and **L_2** (5×10^{-3} M) were prepared in DMSO. For the titration experiments, a 1×10^{-3} M solution of **L_1** taken in a quartz optical cell of 1 cm optical path length was titrated with incremental concentration of anion stock solutions in an ethanolic buffer medium (1:1 v/v EtOH : HEPES buffer at pH 7.2). For the competitive selectivity experiment, fluorescence emission of the **L_1**-Zn^{2+} ensemble was collected in the absence and presence of the competitive metal ions in excess (10 equivalent).

Evaluation of the Apparent Binding Constant

Probe **L_1** at a concentration of 10 μM in buffered ethanol was used for the titration studies with Zn^{2+} solution. The effective Zn^{2+} concentration was varied between 0 and 70 μM and the pH of the solution was adjusted to 7.2 using an aqueous HEPES buffer solution of effective concentration of 10 mM. The apparent binding constant for the formation of the respective zinc complex was evaluated using the Benesi−Hildebrand (B−H) plot (equation 1).[54-55]

$$1/(I-I_0) = 1/\{K(I_{max}-I_0)C\} + 1/(I_{max}-I_0) \quad (1)$$

I_0 is the emission intensity of **L_1** at maximum (λ = 510 nm), I is the observed emission intensity at that particular wavelength in the presence of a certain concentration of the analyte (C), I_{max} is the maximum emission intensity value that was obtained at λ = 510 nm during titration with varying analyte concentration, K is the apparent binding constant (M^{-1}) and was determined from the slope of the linear plot. Similarly, the PPi binding constant was also evaluated.

Detection Limit

The detection limit was calculated on the basis of the fluorescence titration. The fluorescence emission spectrum of **L_1** was measured 10 times, and the standard deviation of blank measurement was determined. To gain the slope, the ratio of the fluorescence emission at 510 nm was plotted against the concentration of Zn^{2+} or PPi. The detection limit was calculated using the following equation:

$$\text{Detection limit} = 3\sigma/k \quad (2)$$

where σ is the standard deviation of blank measurement, and k is the slope between the ratio of fluorescence emission versus respective analyte concentration.

Sensing of Zn(II) in Physiological Milieu

To investigate the potential of $\mathbf{L_1}$ as a probe for intracellular detection of Zn^{2+}, the subsequent endeavour was to study its interaction in milieu replicating the conditions relevant in an *in vitro* system. To that end, two proteins were chosen, bovine serum albumin (BSA) and human serum albumin (HSA), and the interaction study between $\mathbf{L_1}$ and Zn^{2+} was studied. Stock solutions of the proteins were prepared at a final concentration of 4 mg/mL. Proteins were then titrated from the stock solution in a cuvette with preformed $\mathbf{L_1}$-Zn^{2+} complex. To further validate the biological importance of $\mathbf{L_1}$, the interaction of $\mathbf{L_1}$ with Zn^{2+} was also studied in simulated body fluid (SBF), whose ionic composition is similar to that of human extracellular fluid. SBF was prepared as reported previously.[56]

Cytotoxic Effect of L_1, L_1-Zn^{2+} and L_1-Zn^{2+}-PPi Ensemble

The cytotoxic effect of $\mathbf{L_1}$ and $\mathbf{L_1}$.Zn^{2+} complex and $\mathbf{L_1}$-Zn^{2+}-PPi ensemble on HeLa cells (human cervical carcinoma cells) were determined by an MTT assay as per the manufacturer instruction (Sigma-Aldrich, MO, USA). HeLa cells were initially cultured in a 25 cm^2 tissue culture flask in DMEM medium supplemented with 10% (v/v) FBS, penicillin (100 μg mL^{-1}) and streptomycin (100 μg mL^{-1}) under a humidified atmosphere of 5% CO_2 until the cells were approximately 90% confluent. Prior to MTT assay, cells were passaged and seeded into 96 well tissue culture plates at a cell density of 10^4 cells per well and incubated with varying concentrations of $\mathbf{L_1}$, $\mathbf{L_1}$-Zn^{2+} complex, $\mathbf{L_1}$-Zn^{2+}-PPi ensemble, Zn^{2+} and PPi solution (15, 30, 60, 90 and 120 μM) and incubated for a period of 24 h under 5% CO_2. Following incubation, the growth media was carefully aspirated, and fresh DMEM containing MTT solution was added to the wells. The plate was incubated for 4 h at 37°C. Subsequently, the supernatant was collected and the insoluble colored formazan product was solubilized in DMSO and its absorbance was measured in a microtiter plate reader (Infinite M200, TECAN, Switzerland) at 550 nm. The assay was performed in six sets for each concentration of the test samples. Data analysis and determination of standard deviation was performed with Microsoft Excel 2013 (Microsoft Corporation). In the MTT assay, the absorbance for the control cells (solvent control) was considered as 100% cell viability and the absorbance for the treated cells was compared to determine % cell viability with respect to the solvent control.

Detection of Intracellular Zn^{2+} and PPi by Imaging

HeLa cells were initially cultured in a 25 cm^2 tissue culture flask containing DMEM medium supplemented with 10% FBS, penicillin (100 μg mL^{-1}) and streptomycin (100 μg mL^{-1}) in a CO_2 incubator. Prior to imaging studies, HeLa cells were seeded into a 6 well plate and grown in DMEM medium at 37°C till 80% confluency. Subsequently, the cells were washed thrice with sterile phosphate buffered saline (PBS), incubated with 15 μM $\mathbf{L_1}$ in DMEM at 37°C for 1 h in a CO_2 incubator and their images were acquired using a fluorescence microscope (Eclipse Ti-U, Nikon, USA) with a filter that allowed green light emission. The cells were further washed with sterile PBS in order to remove excess $\mathbf{L_1}$ and then incubated for 1 h with 30 μM $Zn(ClO_4)_2$ prepared in sterile PBS. The images of the cells were acquired with a fluorescence microscope. The cells were subsequently washed with sterile PBS and then incubated further with 30 μM PPi for 1 h. Following incubation, the images of the cells were again acquired with a fluorescence microscope as mentioned earlier.

Result and discussion

Selective Sensing of Zn(II) in Aqueous Medium by L_1

The photophysical properties of the chemosensor ($\mathbf{L_1}$) was ascertained by UV-visible absorbance and fluorescence emission changes upon addition of various analytes. Absorption spectrum of $\mathbf{L_1}$ (10 μM) in buffered ethanol (1:1 EtOH : 10 mM HEPES, pH~7.2) exhibited an intense band at 333 nm and a weak band around 386 nm, which may be ascribed to intramolecular π–π∗ transition (Fig. 1a). However, addition of Zn^{2+} ion resulted in the formation of new red shifted absorption peaks at 376 nm and 431 nm with a distinct change in the colour of the solution from colorless to yellowish (Inset, Fig. 1a). Incremental addition of Zn^{2+} ion (0-70 μM) to $\mathbf{L_1}$ resulted in a decrease in intensity at 333 nm accompanied by blue shifting of the 386 nm peak to 377 nm, which emerged with increasing intensity (Fig. 1b). Furthermore, higher Zn^{2+} concentration also lead to the manifestation of a broad peak at 431 nm. The isosbestic points at 297 nm, 355 nm and 414 nm indicated the formation of a new zinc complex with 1:1 stoichiometry (Fig. S9). Interestingly, none of the other tested cations, which included biologically relevant metal ions like Na^+, Mg^{2+} and Ca^{2+}, toxic heavy metal ions like Hg^{2+} and Cd^{2+} affected the absorption spectra of $\mathbf{L_1}$. It may also be mentioned that the absorption spectra of the chemosensor $\mathbf{L_1}$ remained unaffected even in presence of other cations such as K^+, Cu^{2+}, Mn^{2+}, Fe^{2+}, Co^{2+}, Ni^{2+}, Ag^+, Pb^{2+} and Al^{3+} (Fig. 1a).

To acquire a nuanced understanding of the binding mechanism, we have also performed fluorescence emission studies and ^1H NMR titrations in presence of Zn^{2+} ion. The naked probe $\mathbf{L_1}$ (10 μM) was weakly fluorescent at 510 nm perhaps due to rapid rotation around single bond adjacent to azo methine group (λ_{ex} = 430 nm, slit = 3/3 nm). Interaction with Zn^{2+} resulted in a significant Stokes shift of around 130 nm and a remarkable enhancement of the fluorescence emission peak at around 510 (Fig. 2a). Interaction of $\mathbf{L_1}$ with the other tested metal ions failed to impart any change in the

fluorescence emission of the probe (Fig. 2a). Interestingly, under a UV lamp (λ = 365 nm) the solution displayed a strong yellowish green fluorescence (Inset, Fig. 2a) and thus rendered rapid naked eye detection of Zn^{2+}. Collectively the results are encouraging as chemosensors, which exhibit large stokes shift and manifold enhancement in fluorescence upon binding of target analyte are envisaged as potential candidates for fabrication of sensing devices that minimize background interference.

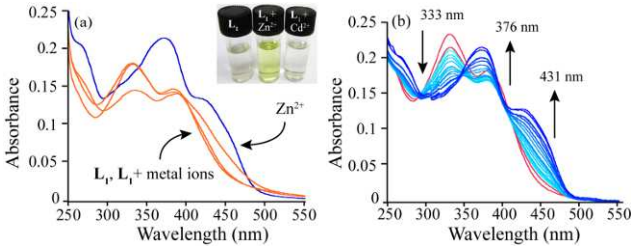

Fig. 1 (a) Change in absorption spectra of $\mathbf{L_1}$ (10 μM) with different metal ions (50 μM) in ethanol buffer mixed buffered solution. INSET: Change in the colour of $\mathbf{L_1}$ solution after the addition of Zn^{2+} and Cd^{2+}. (b) UV-Vis titration spectra of $\mathbf{L_1}$ with increasing Zn^{2+} ion concentration.

To explore the binding mechanism, we have titrated a fixed concentration of the probe (10 μM) with varying concentration of Zn^{2+} ion. With increasing concentration of Zn^{2+} there was a systematic enhancement in the fluorescence emission at 510 nm. Following addition of 0.1 equivalent of Zn^{2+} (1.0 μM of Zn^{2+}), there was nearly 27 fold increase in the fluorescence intensity of the probe (Fig. S10). It may also be mentioned that a noticeable enhancement in the fluorescence intensity of $\mathbf{L_1}$ was even observed with 1.0 nM Zn^{2+}, which indicated the excellent sensitivity of the probe (Fig. 2b). The binding constant for Zn^{2+} ion was 1.25×10^5 M^{-1} as calculated by Benesi- Hildebrand equation using the fluorescence titration reading (Fig. S11a). The calculated lowest detection limit for Zn^{2+} was 71 ppb on the basis of signal: noise = 3:1 (Fig. S11b). In comparison with the reported examples of fluorescent sensors for Zn^{2+} (Table S1, S2), we have achieved better detection limit. Again, such level of detection limit bears significant implications to sense Zn^{2+} in biological systems.

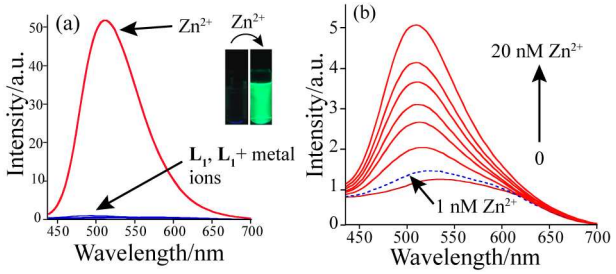

Fig. 2 (a) Emission intensities of $\mathbf{L_1}$ (10 μM) in presence of various metal ions in mixed buffered solution. INSET: Change in colour of $\mathbf{L_1}$ solution observed under a UV lamp following addition of Zn^{2+}. (b) Fluorescence titration of $\mathbf{L_1}$ with varying concentration of Zn^{2+} (0-20 nM) (λ_{ex} = 430 nm, slit = 3/3 nm).

Subsequently, interference studies were conducted to ascertain the affinity of $\mathbf{L_1}$ for Zn^{2+} in presence of other competitive metal ions. For this, fluorescence emission spectra were recorded after the addition of different metal ion solution to a mixture of 1:1 $\mathbf{L_1}$ and Zn^{2+}. Interestingly, the sensing capability of $\mathbf{L_1}$ for Zn^{2+} was not affected in presence of any of the competing species (Fig. S12).

Plausible Mechanism of Zn^{2+} Sensing

To gain an insight of the chelation mode of zinc ion to $\mathbf{L_1}$, ^{1}H NMR titration were conducted. However, due to the poor solubility of the probe in CD_3OD, titrations were performed in DMSO-d_6 (Fig. 3). There are three possible binding sites in $\mathbf{L_1}$ viz. OH, Schiff base N and N of benzothiazole group; and Zn^{2+} coordination through this functionalities are expected to change the nearby electronic environment. Just Following addition of the first aliquot of Zn^{2+} ion, the OH peak was obliterated, which suggested the strong involvement of the OH functionality in the binding event (Fig. 3). Interaction with the Zn^{2+} ion also caused de-shielding of the schiff base CH(Hb) and the aromatic CHs of the benzothiazole ring.

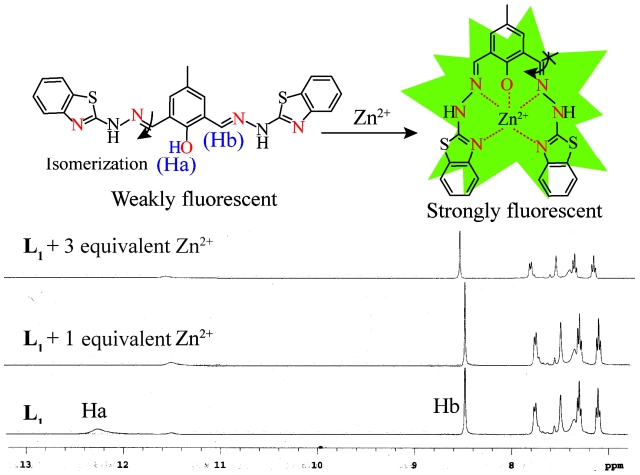

Fig. 3 ^{1}H NMR stack plot of $\mathbf{L_1}$ with different concentration of Zn^{2+} in DMSO-d_6 and the plausible Zn^{2+} binding on top.

A control receptor $\mathbf{L_2}$ which was devoid of OH group also revealed the importance of the same, as it failed to produce any selectivity under the same experimental condition (Fig. S13). Further, the 1:1 complex mass ($\mathbf{L_1}$+Zn^{2+}+NO_3^- = 584.0234, Fig. S14) also suggested the involvement of OH as oxide.

Thus, guided by the phenolic OH, Schiff base N and bezothiazole N are also coordinated to Zn^{2+} ion, and thereby rigidify the molecular assembly by restricting the free rotation of the azomethine carbon, which resulted in significant fluorescent enhancement through the process of chelation-enhanced fluorescence (CHEF).

To test the sensing potential of the developed probe in biological system, it was important to ascertain the performance of the probe in presence of serum proteins such

as albumin.[57] Thus, the Zn^{2+} sensing by $\mathbf{L_1}$ was analyzed in presence of human serum albumin (HSA) and bovine serum albumin (BSA) in mixed solvent system as well as in simulated body fluid (SBF) by tracking the fluorescence emission at 510 nm (Fig. 4). Interestingly, even in presence of higher concentration of HSA, BSA and SBF the fluorescence emission intensity of $\mathbf{L_1}$-Zn^{2+} at 510 nm remained unaffected. These results reiterated the selectivity of the developed probe and demonstrated its application potential in a physiologically relevant milieu.

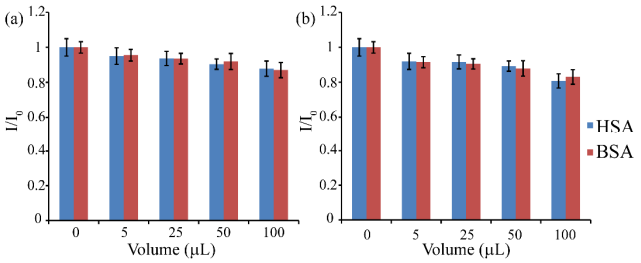

Fig. 4 Histogram showing the fluorescence response of $\mathbf{L_1}$-Zn^{2+} ensemble towards various concentrations of BSA and HSA in (a) buffered ethanol (1:1:: EtOH: :10mM HEPES, pH~7.2) and (b) simulated body fluid (SBF).

Given that chemosensors can exhibit proton-induced fluorescence, the zinc ion induced 'turn-on' fluorescence of $\mathbf{L_1}$ was also checked in a wide pH range. It was observed that $\mathbf{L_1}$ rendered Zn^{2+} sensing in the pH range 5.0 to 11 (Fig. S15). In the pH range <5.0, there was no fluorescence response to Zn^{2+} which may perhaps be attributed to the weak coordination capability of zinc ions due to the protonation of the co-ordination sites of $\mathbf{L_1}$.

For practical application of the chemosensor, paper test strips were used for facile and rapid qualitative detection of Zn^{2+} ion. The ligand coated test strips were prepared by immersing the filter papers into a DCM solution of $\mathbf{L_1}$ and then air dried. An intense 'turn-on' fluorescence could be observed under the UV lamp (λ = 365 nm) on spraying a Zn^{2+} solution over the test strips (Fig. S16).

Selective PPi sensing by $\mathbf{L_1}$-Zn^{2+} ensemble

The next endeavour was to ascertain the anion sensing aptitude of the $\mathbf{L_1}$-Zn^{2+} ensemble. To this end, the $\mathbf{L_1}$-Zn^{2+} ensemble was treated with various anions such as F^-, Cl^-, Br^-, I^-, CN^-, CO_3^{2-}, HCO_3^-, $CH_3CO_2^-$ (OAc^-), NO_3^-, PPi, SO_4^{2-}, PO_4^{3-}, $H_2PO_4^-$, AMP, ADP and ATP etc. Among the aforesaid anions, only PPi induced a conspicuous change in the emissive behaviour of the ensemble (Fig. 5a). Again, the addition of dNTP (N = A, G, C, T) also produce no change in the emissive behavior of the ensemble. Addition of 1.0 equivalent of PPi (10 μM) solution resulted in complete quenching of the initial fluorescence emission of the $\mathbf{L_1}$-Zn^{2+} ensemble. Titration of the metal ensemble with sequentially added PPi solution lead to a continuous decrease in emission intensity at 510 nm. The 'turn-off' fluorescence behaviour of the $\mathbf{L_1}$-Zn^{2+} ensemble could be explained by considering the strong binding affinity of PPi towards Zn^{2+}. The sequestration of Zn^{2+} ions by PPi and formation of stable ZnPPi adduct releases the free probe in the solution, which renders the strong emission of the $\mathbf{L_1}$-Zn^{2+} ensemble.

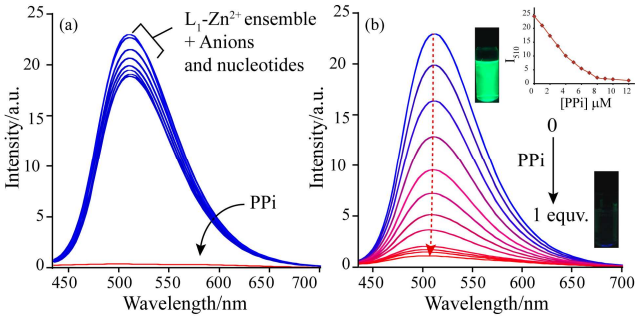

Fig. 5 Change in fluorescence emission upon addition of (a) different anions and (b) increasing concentration of PPi (0 – 10 μM) to the $\mathbf{L_1}$-Zn^{2+} ensemble ion in mixed buffered solution (λ_{ex} = 430 nm, slit = 3/3 nm). INSET: Change of fluorescence emission intensity of the $\mathbf{L_1}$-Zn^{2+} ensemble at 510 nm with increasing concentrations of PPi.

The UV-Vis spectral pattern further validated our conjecture, as absorption maximum at 380 nm for naked $\mathbf{L_1}$ re-emerges was regained and the characteristic 431 nm peak for the zinc ensemble diminished after PPi addition (Fig. S17). Concurrently, the yellowish color solution was also transformed to the original colorless solution. However, neither any visual color change nor any development of new peak around 380 nm was observed in the UV-visible absorbance spectra after addition of any of the anions viz. F^-, Cl^-, Br^-, I^-, CO_3^{2-}, HCO_3^-, OAc^-, NO_3^-, SO_4^{2-}, PO_4^{3-}, $H_2PO_4^-$ even at higher mole ratio. This indicated the high selectivity of the $\mathbf{L_1}$-Zn^{2+} ensemble for PPi ion in the physiological pH. It may also be mentioned that the aforementioned anions could not be detected by the free probe $\mathbf{L_1}$ (Fig. S18). Thus the $\mathbf{L_1}$-Zn^{2+} ensemble can be employed both as colorimetric as well as fluorometric sensor for PPi.

The Job's plot obtained from the titration experiment suggested a 1:1 binding of PPi with metal ensemble and the calculated binding constant was 1.4×10^5 M^{-1} (B-S equation, Fig. S19). The LOD of the zinc ensemble for PPi anion was 480 pM (Fig. S20). To establish the practical applicability of the $\mathbf{L_1}$-Zn^{2+} ensemble as selective PPi sensor, competitive fluorescence experiment was carried out with the competing anions. Addition of PPi caused a prominent fluorescence quenching in every case (Fig. S21), which suggested excellent selectivity and sensitivity of $\mathbf{L_1}$-Zn^{2+} ensemble towards PPi in the buffer medium even in the presence of other interfering anions.

Detection of Zn^{2+} in Live Cells

The results obtained from the fluorescence experiments were encouraging and we sought to investigate the potential of $\mathbf{L_1}$ as a probe for detection of intracellular Zn^{2+}. However, prior to ligand- mediated zinc detection in live cells, it was important to determine its cytotoxic potential. To that end, a an MTT assay was performed. It was observed that that probe alone failed to impart any adverse effect on the

viability of HeLa cells at a concentration of 60 μM (Fig. S22). Even at high concentrations of 90 μM and 120 μM, cell viability was around 80%. Akin to the results obtained with $\mathbf{L_1}$, HeLa cells treated with $\mathbf{L_1}$-Zn^{2+} and $\mathbf{L_1}$-Zn^{2+}-PPi ensembles also displayed significant viability, which suggested high biocompatibility of the ensembles.

The non-toxic nature of the developed chemosensor $\mathbf{L_1}$ and its Zn^{2+}-ensemble suggested that the probe could perhaps be deployed for fluorescence-based intracellular detection of Zn^{2+} in live cells. Therefore, to ascertain the potential of $\mathbf{L_1}$ in intracellular sensing of Zn^{2+}, HeLa cells were incubated with 15 μM $\mathbf{L_1}$ followed by 30 μM of $Zn(ClO_4)_2$ to promote the formation of intracellular $\mathbf{L_1}$-Zn^{2+} complex. It was observed that $\mathbf{L_1}$ alone failed to elicit any fluorescence signals as evidenced by the absence of any intracellular fluorescence (Fig. 6). However, addition of zinc led to the manifestation of bright green fluorescence in HeLa cells (Fig. 6). The fluorescence microscopic analysis strongly suggested that compound $\mathbf{L_1}$ could readily cross the cell membrane, infuse into HeLa cells, and sense Zn^{2+} through the formation of intracellular $\mathbf{L_1}$-zinc complex. It must be also mentioned that bright field images suggested that HeLa cells retained their characteristic morphology, which reiterated the biocompatibility of $\mathbf{L_1}$ and $\mathbf{L_1}$-Zn^{2+} ensemble (Fig. 6). Interestingly, subsequent incubation of the cells with excess PPi resulted in a dramatic loss of fluorescence (Fig. 6), perhaps originating from fluorescence quenching behavior of PPi on $\mathbf{L_1}$-Zn^{2+} ensemble as evidenced from previous solution-based studies (Fig. 5).

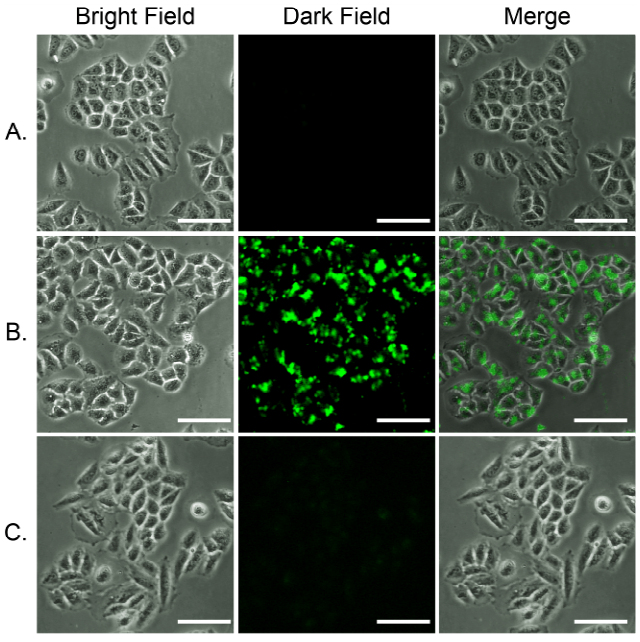

Fig. 6 Fluorescence microscopic images of HeLa cells after adding 15 μM of $\mathbf{L_1}$ (row A) and after subsequent treatment with 30 μM Zn^{2+} (row B) and 30 μM PPi (row C). Scale bar for the images is 100 μm.

Conclusions

A novel benzothiazole containing Schiff base was developed which rendered relay recognition of Zn^{2+} and PPi in physiological medium. The Zn^{2+} sensing was evidenced in mixed buffered medium and also in the physiological milieu in presence of HSA, BSA and SBF. In presence of Zn^{2+}, the colorless chemosensor solution displayed a strong greenish fluorescence and thus enabled naked eye detection of the metal. The chemosensor exhibited a strong affinity ($K = 1.25\times10^5\ M^{-1}$) for Zn^{2+} even in the presence of the other interfering metal ions and was ultrasensitive as it could respond even to 1 nM Zn^{2+} (LOD for Zn^{2+} = 71 ppb). A facile application of the chemosensor could be demonstrated through successful detection of Zn^{2+} using the sensor-coated paper strips. The Zn^{2+}-chemosensor ensemble also responded to PPi in the same experimental medium through fluorescence quenching. On the basis of the selectivity of $\mathbf{L_1}$ for Zn^{2+} in physiological medium and its biocompatible attribute, the probe could facilitate fluorescence-based sensing of intracellular Zn^{2+} in live HeLa cells. It is envisaged that the developed probe holds considerable potential as a Zn^{2+} sensor for future environmental and biomedical applications.

Acknowledgements

The authors thank CSIR (01/2727/13/EMR-II), Science & Engineering Research Board (SR/S1/OC-62/2011) and Department of Biotechnology (BT/01/NE/PS/08), India for financial support and CIF, IIT Guwahati for providing instrument facilities. AG and SM acknowledge IIT Guwahati for research fellowship.

Notes and references

[a]*Department of Chemistry, Indian Institute of Technology Guwahati, Guwahati 781039, India. Fax: + 91 361 2582349; Tel: +91 3612582313; E-mail: gdas@iitg.ernet.in.*
[b]*Department of Biosciences and Bioengineering, Indian Institute of Technology Guwahati, Guwahati, 781039, India. Fax: + 91 361 2582249; Tel: +91 3612582205; E-mail: aramesh@iitg.erent.in.*
Electronic Supplementary Information (ESI) available: [NMR, UV-Vis and fluorescence changes. See DOI: 10.1039/b000000x/]

1. E. L. Que, D. W. Domaille and C. J. Chang, *Chem. Rev.*, 2008, **108**, 1517-1549.
2. R. M.-Manez and F. Sancenon, *Chem. Rev.*, 2003, **103**, 4419-4476.
3. J. S. Kim and D. T. Quang, *Chem. Rev.*, 2007, **107**, 3780-3799.
4. A. P. de Silva, D. B. Fox, A. J. M. Huxley and T. S. Moody, *Coord. Chem. Rev.*, 2000, **205**, 41-57.
5. M. M. Henary, Y. Wu and C. J. Fahrni, *Chem.–Eur. J.*, 2004, **10**, 3015-3025.
6. B. L. Vallee and K. H. Falchuk, *Psychol. Rep.*, 1993, **73**, 79.
7. A. Q. Truong-Tran, J. Carter, R. E. Ruffin and P. D. Zalewski, *Biometals*, 2001, **14**, 315−330.

8. P. D. Zalewski, I. J. Forbes, R. F. Seamark, R. Borlinghaus, W. H. Betts, S. F. Lincoln and A. D. Ward, *Chem. Biol*., 1994, **1**, 153−161.
9. E. Kimura, S. Aoki, E. Kikuta and T. Koike, *Proc. Natl. Acad. Sci*. U.S.A., 2003, **100**, 3731−3736.
10. J. M. Berg and Y. Shi, *Science*, 1996, **271**, 1081-1085.
11. R. Sladek, G. Rocheleau, J. Rung, C. Dina, L. Shen, D. Serre, P. Boutin, D. Vincent, A. Belisle, S. Hadjadj, B. Balkau, B. Heude, G. Charpentier, T. J. Hudson, A. Montpetit, A. V. Pshezhetsky, M. Prentki, B. I. Posner, D. J. Balding, D. Meyre, C. Polychronakos and P. Froguel, *Nature*, 2007, **445**, 881–885.
12. T. Nicolson, E. Bellomo and N. Wijesekara, *Diabetes*, 2009, **58**, 881–885.
13. M.-C. Franz, P. Anderle, M. Burzle, Y. Suzuki, M. R. Freeman, M. A. Hediger and G. Kovacs, *Mol. Aspects Med*., 2013, **34**, 735–741.
14. L. C. Costello and R. B. Franklin, *J. Biol. Inorg. Chem*., 2011, **16**, 3–8.
15. C. L. F. Walker, Z. A. Bhutta, N. Bhandari, T. Teka, F. Shahid, S. Taneja and R. E. Black, *Am. J. Clin. Nutr.,* 2007, **85**, 887–894.
16. C. F. Walker and R. E. Black, *Annu. Rev. Nutr*., 2004, **24**, 255–275.
17. I. Lengyel, J. M. Flinn, T. Peto, D. H. Linkous, K. Cano, A. C. Bird, A. Lanzirotti, C. J. Fredrickson and F. J. G. M. Van Kuijk, *Exp. Eye Res*., 2007, **84**, 772–780.
18. S. K. Ghosh, P. Kim, X. Zhang, S.-H. Yun, A. Moore, S. J. Lippard and Z. Medarova, *Cancer Res*., 2010, **70**, 6119–6127.
19. R. Sladek, G. Rocheleau, J. Rung, C. Dina, L. Shen, D. Serre, P. Boutin, D. Vincent, A. Belisle, S. Hadjadj, B. Balkau, B. Heude, G. Charpentier, T. J. Hudson, A. Montpetit, A. V. Pshezhetsky, M. Prentki, B. I. Posner, D. J. Balding, D. Meyre, C. Polychronakos and P. Froguel, *Nature*, 2007, **445**, 881–885.
20. M. D. Pluth, E. Tomat and S. J. Lippard, *Annu. Rev. Biochem*., 2011, **80**, 333–355.
21. K. M. Dean, Y. Qin and A. E. Palmer, *Biochim. Biophys. Acta*, 2012, **1823**, 1406–1415.
22. D. Karak, S. Das, S. Lohar, A. Banerjee, A. Sahana, I. Hauli, S. K. Mukhopadhyay, D. A. Safin, M. G. Babashkina, M. Bolte, Y. Garcia and D. Das, *Dalton Trans*., 2013, **42**, 6708–6715.
23. Z. Dong, X. Le, P. Zhou, C. Dong and J. Ma, *New J. Chem*., 2014, **38**, 1802-1808.
24. V. Luxami, K. Paul and I. H. Jeong, *Dalton Trans*., 2013, **42**, 3783-3786.
25. S. Kaur, V. Bhalla and M. Kumar, *Chem. Commun*., 2014, **50,** 9725-9728.
26. M. E. Germain and M. J. Knapp, *J. Am. Chem. Soc*., 2008, **130**, 5422-5423.
27. M. E. Germain, T. R. Vargo, P. G. Khalifah and M. J. Knapp, *Inorg. Chem*., 2007, **46**, 4422-4429.
28. S. Kaur, V. Bhalla and M. Kumar, *Chem. Commun*., 2014, **50**, 9725-9728.
29. M. W. Bowler, M. J. Cliff, J. P. Waltho and G. M. Blackburn, *New J. Chem*., 2010, **34**, 784-794.
30. A. K. Hirsch, F. R. Fischer and F. Diederich, *Angew. Chem., Int. Ed.,* 2007, **46**, 338-352.
31. S. K. Kim, D. H. Lee, J.-I. Hong and J. Yoon, *Acc. Chem. Res*., 2009, **42**, 23-31.
32. P. Nyren, *Anal. Biochem*., 1987, **167**, 235-238.
33. S. Xu, M. He, H. Yu, X. Cai, X. Tan, B. Lu and B. Shu, *Anal. Biochem*., 2001, **299**, 188-193.
34. M. Doherty, C. Becher, M. Regan, A. Jones and J. Ledingham, *Ann. Rheum. Dis*., 1996, **66**, 432-436.
35. A. E. Timms, Y. Zhang, R. G. G. Russell and M. A. Brown, *Rheumatology*, 2002, **41**, 725-729.
36. L. Hessle, K. A. Johnson, H. C. Anderson, S. Narisawa, A. Sali, J. W. Goding, R. Terkeltaub and J. L. Millan, *Proc. Natl. Acad. Sci. U. S. A*., 2002, **99**, 9445-9449.
37. C. Beck, H. Morbach, M. Stenzel, H. Collmann, P. Schneider and H. J. Girschick, *Open Bone J*., 2009, **1**, 8-15.
38. P. Das, S. Bhattacharya, S. Mishra and A. Das, *Chem. Commun*., 2011, **47**, 8118–8120.
39. E. J. ONeil and B. D. Smith. *Coord. Chem. Rev*., 2006, **250**, 3068−3080.
40. R. K. Pathak, K. Tabbasum, A. Rai, D. Panda and C. P. Rao, *Anal. Chem*., 2012, **84**, 5117-5123
41. B. Roy, A. S. Rao and K. H. Ahn, *Org. Biomol. Chem*., 2011, **9**, 7774-7779.
42. R. M.-Manez and F. Sancenon, *Chem. Rev*., 2003, **103**, 4419−4476.
43. M. Ronaghi, M. Uhlen and P. Nyren, *Science,* 1998, **281**, 363–365.
44. I. S. Shin, S. W. Bae, H. Kim and J. I. Hong, *Anal. Chem*., 2010, **82**, 8259–8265.
45. M. J. Rothberg, W. Hinz, L. K. Johnson, M. J. Bustillo, H. J. Leamon and J. Schultz, *PCT Int. Appl.,* 2010, WO 2010008480 A2 20100121.
46. A. Gogoi, S. Samanta and G. Das, *Sens. Actuators, B*, 2014, **202**, 788-794.
47. B. K. Datta, D. Thiyagarajan, S. Samanta, A. Ramesh and G. Das, *Org. Biomol. Chem*., 2014, **12**, 4975-4982.
48. B. K. Datta, S. Mukherjee, C. Kar, A. Ramesh and G. Das, *Anal. Chem*., 2013, **85**, 8369–8375.
49. A. Gogoi, S. Mukherjee, A. Ramesh and G. Das, *Anal. Chem*., 10.1021/acs.analchem.5b01746.
50. Z. Dong, X. Le, P. Zhou, C. Dong and J. Ma, *RSC Adv*., 2014, **4**, 18270–18277.
51. C. Kar, M. D. Adhikari, B. K. Datta, A. Ramesh and G. Das, *Sens. Actuators, B,* 2013, **188**, 1132– 1140.
52. S. Anbu, R. Ravishankaran, M. F. C. Guedes da Silva, A. A. Karande and A. J. L. Pombeiro, *Inorg. Chem*., 2014, **53**, 6655–6664.
53. S. Anbu, S. Kamalraj, C. Jayabaskaran and P. S. Mukherjee, *Inorg. Chem*., 2013, **52**, 8294–8296.
54. H. A. Benesi and J. H. Hildebrand, *J. Am. Chem. Soc*., 1949, **71**, 2703-2707.

55. F. Han, Y. Bao, Z. Yang, T. M. Fyles, J. Zhao, X. Peng, J. Fan, Y. Wu and S. Sun, *Chem. Eur. J.,* 2007, **13**, 2880-2892.
56. A. Oyane, H. M. Kim, T. Furuya, T. Kokubo, T. Miyazaki and T. Nakamura, *J. Biomed. Mater. Res*., 2003, **65**, 188-195.
57. R. K. Pathak, A. G. Dikundwar, T. N. G. Row and C. P. Rao, *Chem. Commun*., 2010, **46**, 4345–4347.

